

A Contribution to the Theory of Corrugated Guides¹

G. Piefke

(January 25, 1960)

The transmission characteristics of certain structures belonging to the class of corrugated guides are calculated by means of a new method. It is assumed that the guide wavelength always is much greater than the corrugation constant ($D_1 + D_2$ in fig. 1). The periodical structure of the guide is therefore replaced by a quasi-homogeneous, but anisotropic medium.

The following structures are studied: The "ring-element guide," which consists of an axial stack of insulated metallic rings with arbitrary surrounding medium; the "disk guide," which is a ring-element guide with infinite radial extension of the rings; the "disk loaded waveguide," and the "corrugated waveguide."

As a rule guides can propagate modes with a phase velocity $v_p > c$ (c = velocity of light) and modes with $v_p < c$. The capability of existence of the various modes depends on the losses of the guide. The ring-element guide is well suited for transmission with the H_{01} -mode since, except the H_{0n} -modes, all modes may be highly attenuated (mode filters). As delay lines ($v_p < c$), all guides have band pass characteristics.

1. Introduction

Many periodic structures can be classified under the heading "corrugated guides." In this class are, for instance, the "disk guide," the "disk loaded waveguide," the "corrugated waveguide," the wire fitted with annular grooves and the "ring-element guide" (figs. 1 to 5). These types of guide have many potentialities in communications.

The disk guide (fig. 1) which consists of an axial stack of insulated metallic rings of such radial dimension that no electromagnetic field can exist outside the rings, can be used as a transmission path for the H_{01} -mode. Of the H_{01} -mode in the circular waveguide, it is known that its attenuation decreases with increasing frequency. An attenuation sufficiently low for communication purposes is obtained, however, only for a wavelength small with respect to the guide diameter. With an inner diameter of the circular waveguide of 5 cm and a wavelength $\lambda_0 = 6$ mm the attenuation of the H_{01} -mode is 0.134 N/km. With sufficiently small attenuation of the H_{01} -mode many other modes are capable of existence in the waveguide, however. These undesired modes can be excited by the H_{01} -mode, if at any place the waveguide deviates from its round and straight form. Such undesired modes, however, have a velocity other than the H_{01} -mode and the next inhomogeneity of the waveguide converts part of them back to the H_{01} -mode so that signal distortion comes about. By strong attenuation of the parasitic modes such reconversion and resultant signal distortion can be avoided. With transmission by means of the H_{01} -mode a guide is thus desired along which the H_{01} -mode has the same propagating properties as in a circular homogeneous waveguide and where the undesired modes are strongly attenuated. This is possible with the disk guide.

The disk loaded waveguide (fig. 2) is used as a linear accelerator. The corrugated waveguide (fig. 3) is used as a flexible waveguide. The wire with annular grooves (fig. 4) presents, if the groove depth is small with respect to the wavelength, similar properties as the Goubau guide and, if it is large, it can likewise serve as a delay line. Like the disk guide the ring-element guide (fig. 5) consists of an axial stack of insulated metallic rings, but it has another arbitrary outer medium and therefore an electromagnetic field is possible also outside the rings.

The ring-element guide is thus a generalization of the disk guide and the disk loaded waveguide, and it can likewise be used for transmission with the H_{01} -mode.

¹ Contribution from the Central Laboratories of the Siemens & Halske AG, Munich, Germany.

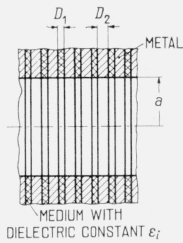


FIGURE 1. Disk guide.

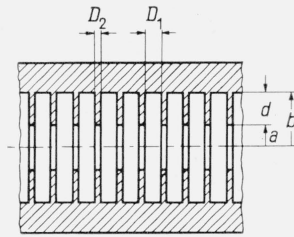


FIGURE 2. Disk loaded waveguide.

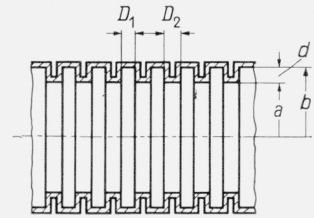


FIGURE 3. Corrugated waveguide.

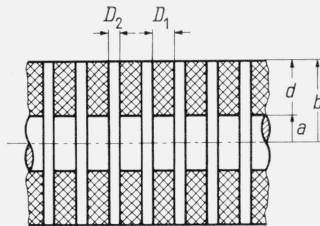


FIGURE 4. Wire with annular grooves.

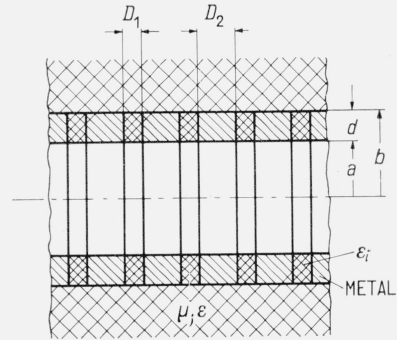


FIGURE 5. Ring-element guide.

The paper [1]² gives a good review of the principal theories known so far concerning corrugated guides. The papers [2] to [5] deserve to be mentioned in particular as individual articles. Because of the complicated boundary conditions an exact solution of Maxwell's equations is very difficult with corrugated guides.

For the case that the corrugation constant is far smaller than the guide wavelength ($D_1 + D_2 \ll \lambda$), the author has used in the papers [6] to [8] a new method of calculating the transmission characteristics of corrugated guides. It introduces a quasi-homogeneous, but anisotropic medium and offers the advantage that in each region Maxwell's equations can be solved easily and the boundary conditions can be met with ease.

In this paper the mathematical method shall be briefly recapitulated and the results of the papers [6] to [8] summarized.

2. Mathematical Approach

Let us consider the disk guide of figure 1. For the disk separation $D_1 + D_2$, the thickness D_1 of the dielectric, and the axial thickness D_2 of the disks there shall hold the inequalities

$$D_1 + D_2 \ll \lambda, \quad (1)^3$$

$$D_1 \ll \frac{1}{2} \lambda_0 \sqrt{|\epsilon_0 / \epsilon_i|}, \quad (2)$$

$$D_2 \gg \vartheta. \quad (3)$$

The medium in the region $a < r < \infty$, which is termed medium 1 herein has a periodic structure with respect to the axial coordinate z and therefore is inhomogeneous. Besides the medium has a different structure in the direction z than in the directions φ and r . The medium is therefore anisotropic as well.

² Figures in brackets indicate the literature references at the end of this paper.

³ A list at the end of this paper explains the symbols.

If a mode is excited in the region $0 < r < a$ (medium 0), the medium 1 can be considered as quasi-homogeneous because of the inequality (1). Dielectric constant and permeability of this quasi-homogeneous, but anisotropic medium 1 are found from the following consideration (see also [6] and [9]).

If the mode excited in medium 0 has an electric field only in a circular direction and a magnetic field in the axial and radial directions (H_{0n} -mode), no energy will be capable of propagating in the direction r , because of the inequality (2). At the place $r=a$ current will flow in a circular direction. For this current, i.e., in parallel to the disk, the medium 1 is a conductor with the conductivity

$$\kappa_p = \kappa \frac{D_2}{D_1 + D_2} \quad (4)$$

or the dielectric constant

$$\epsilon_p = \kappa_p / j\omega. \quad (5)$$

The permeability in the direction z , i.e., perpendicularly to the disks, is given by the permeability of the dielectric and that of the metal. If dielectric and metal have the permeability μ_0 of space, there holds accordingly

$$\mu_z = \mu_0. \quad (6)$$

If the mode excited in medium 0 has a magnetic field only in a circular direction, and an electrical field in axial and radial directions (E_{0n} -mode), energy is capable of propagating between the disks in the direction r . Because of inequality (3), the metal is field-free. Perpendicularly to the disks the medium 1 therefore has the dielectric constant

$$\epsilon_z = \epsilon_i \frac{D_1 + D_2}{D_1}, \quad (7)$$

and in parallel to them the permeability

$$\mu_p = \mu_0 \frac{D_1}{D_1 + D_2}. \quad (8)$$

Since medium 1 has the same structure in the directions φ and r , the dielectric constant ϵ_p and the permeability μ_p hold also for the directions φ and r . In the coordinate system r, φ, z , the dielectric constant and the permeability in medium 1 are thus tensors as follows

$$\epsilon_1 = \begin{pmatrix} \epsilon_p & 0 & 0 \\ 0 & \epsilon_p & 0 \\ 0 & 0 & \epsilon_z \end{pmatrix}, \quad (9)$$

$$\mu_1 = \begin{pmatrix} \mu_p & 0 & 0 \\ 0 & \mu_p & 0 \\ 0 & 0 & \mu_0 \end{pmatrix}. \quad (10)$$

In medium 0 the solution of Maxwell's equations is generally known. Because of the eqs (4) to (10) Maxwell's equations can be easily solved also in the medium 1, as shown in [6]. In the same way the boundary conditions at the point $r=a$ can now be satisfied with ease.

In calculating the transmission properties of the ring-element guide, the approach is exactly the same as with the disk guide. The difference is merely the limited extension of the quasi-homogeneous anisotropic medium which in turn is surrounded by an arbitrary outer medium. The ring-element guide thus is the more general case. The disk-loaded waveguide develops from the ring-element guide, if the outer medium is a conductor.

Because of the general importance of the ring-element guide the equation set up in [7] for calculating the propagation constants of the individual modes has been stated once more in the eqs (83) and (84) of the annex.

3. General Considerations

With all forms of guide shown in figs. 1 to 5, unlike waveguides, each mode type is a combination of an E -mode and an H -mode, even when losses are neglected. An exception is merely the rotation-symmetrical modes. Accordingly the modes with $m \neq 0$ are here termed HE -modes or EH -modes. The first letter identifies always the mode type that prevails. With the HE -modes the H -type thus prevails and with the EH -modes the E -type.

Only the rotation-symmetrical H -modes have thus no axial electric field. As mentioned above, no energy can thus be transported by these modes between the rings in the direction r ; energy will penetrate into medium 1 merely corresponding to the conductivity κ_p .

With the other modes, however, plenty of energy can penetrate into medium 1 because of the presence of the axial electric field. If the dielectric between the rings has no losses and if those of the metal are neglected, modes will propagate between the rings in a radial direction without attenuation. With the disk guide these modes receive power from the mode traveling in the region $0 < r < a$, as figure 6 shows. In medium 1 the connecting line of the points of equal phase is oblique with respect to the axis z . There exists an axial and a radial phase velocity. This fact corresponds also to the solution of Maxwell's equations in the anisotropic medium 1, where a mode propagating in the directions r and z is obtained although the thickness of the metallic disks has been assumed as very large with respect to that of the equivalent conducting layer. With the lossless disk guide all modes with an axial electric field thus are attenuated by radiation.

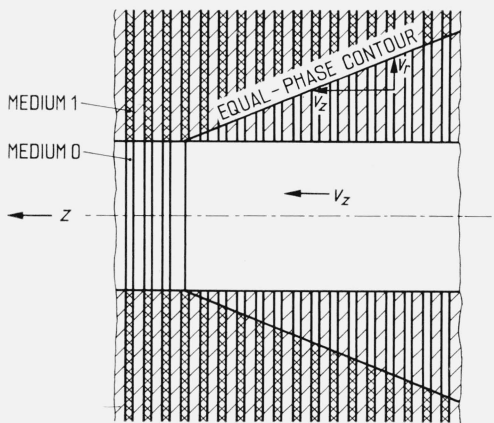


FIGURE 6. Generation of the radial modes in the disk guide with a mode propagating in the z -direction (schematic; v_z is the axial, v_r the radial phase velocity in medium 1).

It is advisable to classify the mode types in the here considered guide forms by phase velocities, for there exist as well mode types whose phase velocity v_p exceeds the velocity of light c , as others whose phase velocity v_p is less. Modes with a phase velocity $v_p > c$ are termed herein as a rule "waveguide modes" and may be HE_{mn} -modes as well as EH_{mn} -modes. In the same way as with circular waveguides, the subscript m here refers to the circular, and the subscript n to the radial dependence of the field. Modes with a phase velocity $v_p < c$ give the guide the character of a delay line and can be only EH_m -modes. The subscript n is here dropped as a rule, for in this case, unlike the waveguide modes, there exists for each m only one mode with a particular field configuration. In exceptional cases $v_p > c$ is possible even with the EH_m -modes.

An essential point with the modes is their capability of existence; with the modes with $v_p > c$ it differs from that with the modes with $v_p < c$. With some types of guides it turns out, for instance, that waveguide modes are capable of existence only if the total loss exceeds a certain limit which depends on frequency, mode type, material constants, and dimensions of the respective guide.

As an example for the existence capability of the modes let us now consider the ring-element guide. Neglecting, for instance, the losses due to the rings and the insulation between rings,

only such waveguide modes can exist, with the exception of the H_{0n} -modes, for which

$$(\beta_0 a)^2 \left| \operatorname{Im} \left(\frac{\mu \epsilon}{\mu_0 \epsilon_0} \right) \right| > \left| \operatorname{Im} ([k_0 a]^2) \right|. \quad (11)$$

The eigenvalue $k_0 a$ can be taken from the eqs (13), (18), and (22) to (24).

If the inequality (11) holds, the negative sign must always be chosen with the radial propagation constant in the outer medium that is given by

$$k_2 = \pm \sqrt{\beta_0^2 \frac{\mu \epsilon}{\mu_0 \epsilon_0} + \gamma^2} = \pm \sqrt{\beta_0^2 \left(\frac{\mu \epsilon}{\mu_0 \epsilon_0} - 1 \right) + k_0^2}. \quad (12)$$

The energy then propagates into the outer medium.

If the inequality (11) does not hold, the losses of the rings and the insulation must be also considered, followed by checking whether there results a value k_0 with positive real and imaginary parts and in addition a value k_2 with positive imaginary part. If such is not the case, the respective waveguide mode is not capable of existence. With high losses of the outer medium the inequality (11) is always met and the losses of the rings can be neglected with all waveguide modes except the H_{0n} -modes. Their losses are given by those at the inside of the guide (see eq (31)).

If the outer medium and the dielectric between the rings are free of losses, hence are air for instance, the losses of the rings must be taken into account for checking the existence of the waveguide modes and calculating their losses. The existence of the waveguide modes then depends in turn upon whether the aforementioned conditions for k_0 and k_2 are satisfied. At any rate the positive sign must now be chosen in eq (12), i.e., k_2 has a positive real part and energy flows into the rings from all sides. As a rule, however, the losses of the rings will not suffice to secure the existence of waveguide modes. An exception is merely the H_{0n} -modes which are capable of existence, even if all losses are neglected. Apart from the H_{0n} -modes the loss-free ring-element guide thus has merely modes with $v_p < c$, i.e., E_0 or EH_m -modes ($m \neq 0$) and therefore is a delay line as a rule.

Like waveguide modes, modes with $v_p < c$ are not capable of existence with any outer medium. Examples in point are the disk loaded waveguide and the corrugated waveguide, which develop from the ring-element guide, if the outer medium is metal. In these guides no modes are possible except waveguide modes, if the corrugation depth is small with respect to wavelength λ_0 . Only with a corrugation depth that is large with respect to the wavelength λ_0 waveguide modes are possible as well as modes with $v_p < c$ (see section 6).

If with the ring-element guide the losses of the dielectric between the ring are so large that the fields cannot penetrate beyond the rings, the regions $0 < r < a$ and $b < r < \infty$ are decoupled with respect to each other. For an excitation in the region $0 < r < a$ the ring-element guide acts now as a disk guide. With an excitation in the space $b < r < \infty$ surface modes are obtained on the ring-element guide. Either mode can be calculated from the general eqs (83) and (84). With high losses of the insulation between the rings the ring-element guide thus will act as waveguide or surface mode guide, depending on the excitation. Let us now proceed to a study of the various guide varieties.

4. Ring-Element Guide

4.1. Formulas for the Propagation Constants of the Waveguide Modes

As mentioned above, the ring-element guide is a generalization of the disk guide, disk loaded waveguide, and corrugated waveguide. For this reason let us begin by stating the formulas for the propagation constants of the modes in the ring-element guide. The formulas for the propagation constants of the modes in the other guide types are then obtained as specific cases.

With the ring-element guide no generally valid closed formulas exist for the propagation constants of the modes, but such formulas can be calculated under certain assumptions and the essential properties of the guide can so be explained, as was done in detail in [7].

Under the assumptions

$$k_0 a = \chi + \Theta, \quad |\Theta| \ll 1, \quad (13), (13a)$$

$$\left| \frac{2\chi\Theta}{(\beta_0 a)^2} \right| \ll \left[1 - \left(\frac{\chi}{\beta_0 a} \right)^2 \right] \quad (14)$$

$$\left. \begin{array}{l} \left| \beta_0 b \sqrt{\left(\frac{\mu\epsilon}{\mu_0\epsilon_0} - 1 \right) + \left(\frac{k_0 a}{\beta_0 a} \right)^2} \right| \\ \left| \beta_0 b \sqrt{\frac{\mu\epsilon}{\mu_0\epsilon_0}} \right| \end{array} \right\} \gg \left\{ \begin{array}{l} 1 \\ m \end{array} \right. \quad (15)$$

$m=0,1,2, \text{ etc.},$

there is according to [7]

$$\beta = \beta_0 \sqrt{1 - \left(\frac{\chi}{\beta_0 a} \right)^2} - \frac{\chi}{\beta_0 a^2 \sqrt{1 - \left(\frac{\chi}{\beta_0 a} \right)^2}} \operatorname{Re}(\Theta), \quad (16)$$

$$\alpha = \frac{\chi}{\beta_0 a^2 \sqrt{1 - \left(\frac{\chi}{\beta_0 a} \right)^2}} \operatorname{Im}(\Theta), \quad (17)$$

where

$$\chi = \begin{cases} \sigma_{mn} & \text{for } H\text{- and } HE\text{-modes with } |\Theta_H| \ll \ll 1 \\ \chi_{mn} & \text{for } E\text{- and } EH\text{-modes with } |\Theta_E| \ll \ll 1 \\ \sigma_{mn} & \text{for } E\text{- and } EH\text{-modes with } |\bar{\Theta}_E| \ll \ll 1 \end{cases} \quad (18)$$

$$\Theta = \begin{cases} \Theta_H & \text{for } HE\text{-modes} \\ \Theta_E & \text{for } EH\text{-modes} \\ \bar{\Theta}_E & \text{for } EH\text{-modes for very large } a/\lambda_0. \end{cases} \quad (18a)$$

There denote

$$\Theta_H = j \frac{\sigma_{0n}}{\beta_0 a} \frac{Z_H}{Z_0}, \quad (19)$$

$$\Theta_E = j \frac{\beta_0 a}{\chi_{0n}} \frac{Z_a}{Z_0}, \quad (20)$$

$$\bar{\Theta}_E = j \frac{\sigma_{0n}}{\beta_0 a} \frac{Z_0}{Z_a}, \quad (21)$$

for $m=0, n=1,2,3, \text{ etc.}$

$$\Theta_H = j \frac{\sigma_{mn} Z_0 [1 - \sqrt{1 - F_a(\sigma_{mn})}]}{2\beta_0 a Z_a \left[1 - \left(\frac{m}{\sigma_{mn}} \right)^2 \right]}, \quad (22)$$

$$\Theta_E = j \frac{2\beta_0 a Z_a}{\chi_{mn} Z_0 [1 + \sqrt{1 - F_a(\chi_{mn})}]}, \quad (23)$$

$$\bar{\Theta}_E = j \frac{\sigma_{mn} Z_0 [1 + \sqrt{1 - F_a(\sigma_{mn})}]}{2\beta_0 a Z_a \left[1 - \left(\frac{m}{\sigma_{mn}} \right)^2 \right]}, \quad (24)$$

for $m=1,2,3, \text{ etc.}; n=1,2,3, \text{ etc.}$

The quantities $F_a(\sigma_{mn})$ and $F_a(\chi_{mn})$ are calculated from

$$F_a(\chi) = 4 \left(\frac{Z_a}{Z_0} \right)^2 \left\{ \left(\frac{m}{\chi} \right)^2 \left[\left(\frac{\beta_0 a}{\chi} \right)^2 - 1 \right] + \frac{Z_H}{Z_a} \right\} \quad (25)$$

by replacing χ by the quantities σ_{mn} or χ_{mn} .

There denote further in the eqs (19) to (25)

$$\frac{Z_H}{Z_0} = (1+j) \sqrt{\frac{\beta_0(D_1+D_2)}{2Z_0\kappa D_2}}, \quad (26)$$

$$\frac{Z_a}{Z_0} = \frac{Z_A}{Z_0} \frac{1+j \frac{Z_E}{Z_A} \tan p_E d}{1+j \frac{Z_A}{Z_E} \tan p_E d}, \quad (27)$$

$$\frac{Z_E}{Z_0} = \sqrt{\frac{\epsilon_0}{\epsilon_i}} \frac{D_1}{D_1+D_2}, \quad (28)$$

$$\frac{Z_A}{Z_0} = -\frac{\epsilon_0 k_2}{\epsilon \beta_0} = \frac{\epsilon_0}{\epsilon} \sqrt{\left(\frac{\mu\epsilon}{\mu_0\epsilon_0} - 1\right) + \left(\frac{\chi}{\beta_0 a}\right)^2}. \quad (29)$$

In calculating β and α of the H_{0n} -modes and HE_{mn} -modes with $|\Theta_H| \ll 1$ set $\chi = \sigma_{mn}$ in all equations. The same holds in calculating β and α of the E_{0n} -modes and EH_{mn} -modes with $|\Theta_E| \ll 1$. At very high frequencies, i.e., for large a/λ_0 , the E_{0n} -modes and EH_{mn} -modes thus have the eigenvalue σ_{mn} or rather $\sigma_{m(n-1)}$ ($n \neq 1$) and accordingly a phase constant approaching that of the HE_{mn} -modes or rather $HE_{m(n-1)}$ -modes ($n \neq 1$) (cf. eq (16)), viz, at very high frequencies the electrical field configuration of the E_{0n} -modes and EH_{mn} -modes is practically the same as that of the magnetic field with the corresponding $H_{0(n-1)}$ -modes and $HE_{m(n-1)}$ -modes ($n \neq 1$). In calculating β and α of the customary E_{0n} -modes and EH_{mn} -modes with $|\Theta_E| \ll 1$ there must be set $\chi = \chi_{mn}$ in all equations. Z_H/Z_0 and Z_a/Z_0 give the influence of the wall and the outer medium onto the waveguide modes, for Z_H/Z_0 is the ratio of the radial field characteristic impedance of the wall to that of space with the H_{0n} -modes (see eq (19)). Since these modes have only a circular electric field in parallel to the rings, no field penetrates between the rings, and with Z_H/Z_0 there appears as dielectric constant merely $\epsilon_p = \kappa_p/j\omega$, the outer medium having no influence. According to eq (27) Z_a/Z_0 is the input impedance of a guide terminated into the impedance Z_A , as referred to the field characteristic impedance Z_0 . This guide has here the characteristic impedance Z_E and the electrical length $\sqrt{\epsilon_i/\epsilon_0}d$, if ϵ_i is real. The magnitude Z_a/Z_0 can thus be calculated with the aid of the known Smith chart, where, as a function of d , the aforesaid input impedance lies always on a circle, if ϵ_i is real and the losses in the metal are neglected. In the same way as the quantity Z_H/Z_0 appears with the H_{0n} -modes, the quantity Z_a/Z_0 shows up with the E_{0n} -modes, since they have an axial electric field perpendicularly to the rings and the field therefore can issue between the rings into the outer region (see eqs (20) and (21)). The E_{0n} -modes can thus be affected very heavily by the outer medium. From the eqs (16), (17), and (19) to (21) there results thus for the phase and attenuation constants with the H_{0n} -modes

$$\beta_H = \beta_0 \sqrt{1 - \left(\frac{\sigma_{0n}}{\beta_0 a}\right)^2} + \alpha_H, \quad (30)$$

$$\alpha_H = \sqrt{\frac{D_1+D_2}{D_2}} \alpha_{Hh} \quad (31)$$

and with the E_{0n} -modes

$$\beta_E = \beta_0 \sqrt{1 - \left(\frac{\chi_{0n}}{\beta_0 a}\right)^2} + \frac{1}{a \sqrt{1 - \left(\frac{\chi_{0n}}{\beta_0 a}\right)^2}} \operatorname{Im} \left(\frac{Z_a}{Z_0} \right), \quad (32)$$

$$\alpha_E = \frac{1}{a \sqrt{1 - \left(\frac{\chi_{0n}}{\beta_0 a}\right)^2}} \operatorname{Re} \left(\frac{Z_a}{Z_0} \right), \quad (33)$$

$$\bar{\beta}_E = \beta_0 \sqrt{1 - \left(\frac{\sigma_{0n}}{\beta_0 a}\right)^2} + \frac{1}{a} \left(\frac{\sigma_{0n}}{\beta_0 a}\right)^2 \frac{\operatorname{Im} \left(\frac{Z_0}{Z_a} \right)}{\sqrt{1 - \left(\frac{\sigma_{0n}}{\beta_0 a}\right)^2}}, \quad (34)$$

$$\bar{\alpha}_E = \frac{1}{a} \left(\frac{\sigma_{0n}}{\beta_0 a}\right)^2 \frac{\operatorname{Re} \left(\frac{Z_0}{Z_a} \right)}{\sqrt{1 - \left(\frac{\sigma_{0n}}{\beta_0 a}\right)^2}}. \quad (35)$$

In eq (31) there denotes

$$\alpha_{Hh} = \sqrt{\frac{\beta_0}{2Z_0\kappa}} \frac{1}{a\sqrt{1-\left(\frac{\sigma_{0n}}{\beta_0 a}\right)^2}} \left(\frac{\sigma_{0n}}{\beta_0 a}\right)^2 \quad (36)$$

the attenuation constant of the H_{0n} -modes in the homogeneous waveguide. The phase and attenuation constants β_E and α_E refer to the E_{0n} -modes with $|\Theta_E| \ll 1$. The quantities $\bar{\beta}_E$ and $\bar{\alpha}_E$ relate to the E_{0n} -modes with $|\bar{\Theta}_E| \ll 1$.

With

$$F_a(x) \ll 1 \quad (37)$$

the root in the eqs (23) to (25) can be expanded into a series and after insertion of eqs (22) to (24) into eq (17) there is found

$$\alpha_{HE} = \frac{1}{a} \left(\frac{\sigma_{mn}}{\beta_0 a}\right)^2 \frac{\operatorname{Re}\left(\frac{Z_a}{Z_0} \left\{ \left(\frac{m}{\sigma_{mn}}\right)^2 \left[\left(\frac{\beta_0 a}{\sigma_{mn}}\right)^2 - 1 \right] + \frac{Z_H}{Z_a} \right\}\right)}{\left[1 - \left(\frac{m}{\sigma_{mn}}\right)^2\right] \sqrt{1 - \left(\frac{\sigma_{mn}}{\beta_0 a}\right)^2}} \quad (38)$$

$$\alpha_{EH} = \frac{1}{a\sqrt{1 - \left(\frac{\chi_{mn}}{\beta_0 a}\right)^2}} \operatorname{Re}\left(\frac{Z_a}{Z_0}\right), \quad (39)$$

$$\bar{\alpha}_{EH} = \frac{1}{a} \left(\frac{\sigma_{mn}}{\beta_0 a}\right)^2 \frac{\operatorname{Re}\left(\frac{Z_0}{Z_a}\right)}{\left[1 - \left(\frac{m}{\sigma_{mn}}\right)^2\right] \sqrt{1 - \left(\frac{\sigma_{mn}}{\beta_0 a}\right)^2}}, \quad m=0, 1, 2, \text{ etc.} \quad (40)$$

where α_{HE} the attenuation constant with the HE_{mn} -modes, α_{EH} that with the EH_{mn} -modes ($|\Theta_E| \ll 1$) and $\bar{\alpha}_{EH}$ that with the EH_{mn} -modes with $|\bar{\Theta}_E| \ll 1$.

From the eqs (38) to (40) one obtains also the well-known attenuation formulas of the modes in the homogeneous waveguide, equating $Z_a = Z_H$ and $D_1 = 0$.

An example is to show, when the phase and attenuation constants with horizontal stroke on top hold, hence when the eqs (34), (35), and (40) are valid. With the homogeneous waveguide there is $Z_a = Z_H$ and $D_1 = 0$, as mentioned. There results accordingly from the eqs (20), (21), and (26) $|\Theta_E| = 15.4$ and $|\bar{\Theta}_E| = 0.045$ for the E_{02} -mode in the homogeneous waveguide, i.e., $\chi_{02} = 5.52$ and $\sigma_{01} = 3.83$, with $a = 2.5$ cm, $\lambda_0 = 0.01$ mm, $\kappa = 57 \times 10^4$ mho/cm (copper), i.e., the eqs (34) and (35) are valid. Since Z_a/Z_0 will mostly be greater than Z_H/Z_0 , the eqs (34) and (35) will hold with the ring-element guide even with a wavelength in excess of $\lambda_0 = 0.01$ mm. From the eqs (39) and (40) the following interesting function of the attenuation of the E_{0n} -modes ($n \neq 1$) and EH_{mn} -modes ($n \neq 1$) in the homogeneous waveguide results thus: ($Z_a = Z_H$, $D_1 = 0$). Initially, according to eq (39), starting at a very high value at the cutoff frequency the attenuation decreases with increasing frequency, subsequently it passes through a minimum and rises again. Thereafter the attenuation must pass through a maximum, since, according to eq (40), it decreases again for sufficiently high frequencies. With the ring-element guide the attenuation/frequency curve is basically the same, but additional variations will come about because of the quantity Z_a/Z_0 which, according to eq (27), is approximately periodical as a function of frequency. With respect to the attenuation constants of the H_{0n} -modes of eq (31) there can further be stated that the root term in a certain way takes into account the penetration of the field between the rings and that, because of the inequality (2), the radiation damping can mostly be neglected with the thicknesses d encountered in practice.

As mentioned above, an essential point is the capability of existence of the modes. Inserting eq (13) into the inequality (11) yields that with a real ϵ_i and neglecting of the ring losses there are capable of existence only the E_{0n} -modes, HE_{mn} -modes, and EH_{mn} -modes ($m \neq 0$) for which

$$(\beta_0 a)^2 \left| \operatorname{Im} \left(\frac{\mu \epsilon}{\mu_0 \epsilon_0} \right) \right| > \begin{cases} 2\sigma_{mn} \operatorname{Im}(\Theta_H) \\ 2\chi_{mn} \operatorname{Im}(\Theta_E) \\ 2\sigma_{mn} \operatorname{Im}(\bar{\Theta}_E). \end{cases} \quad (41)$$

4.2. Application of the Ring-Element Guide as a Mode Filter in Transmission With the H_{01} -Mode

The influence of the outer medium onto the waveguide modes is the greater, the stronger the axial electric field of the waveguide modes, i.e., an outer medium with high losses will attenuate the EH_{mn} -modes far more than the HE_{mn} -modes. With use of the ring-element guide as a mode filter in transmission with the H_{01} -mode the attenuation of the EH_{mn} -modes is always sufficient. It is, therefore, important so to design the guide that also the HE_{mn} -modes are attenuated as strongly as possible. In calculating the loss of the HE_{mn} -modes the losses of the rings and the dielectric between them can be neglected, if the outer medium has high losses, i.e., it is possible to set $\kappa = \infty$ and thus $Z_H/Z_0 = 0$. From the eqs (17) and (22) maximum attenuation results then for $F_a(\sigma_{mn}) = 1$, i.e., if Z_a/Z_0 is real and has a certain value. For a real ϵ_i one obtains therefore from the eqs (25), (27), (28), and (29) the following design rules for maximum attenuation of the HE_{mn} -modes:

$$\frac{Z_E}{Z_0} = \sqrt{R \left(U - \frac{V^2}{R-U} \right)}, \quad (42)$$

$$\tan \left(\beta_0 \sqrt{\frac{\epsilon_i}{\epsilon_0}} d \right) = \frac{R-U}{VR} \frac{Z_E}{Z_0}, \quad (43)$$

$$\frac{Z_a}{Z_0} = R = \frac{\sigma_{mn}}{2m \sqrt{\left(\frac{\beta_0 a}{\sigma_{mn}} \right)^2 - 1}}, \quad m, n = 1, 2, 3, \text{ etc.} \quad (44)$$

The quantities U and V are the real and imaginary parts of Z_A/Z_0 and therefore calculated according to eq (29) from

$$\frac{\epsilon_0}{\epsilon} \sqrt{\left(\frac{\mu\epsilon}{\mu_0\epsilon_0} - 1 \right) + \left(\frac{\sigma_{mn}}{\beta_0 a} \right)^2} = U + jV. \quad (45)$$

From the eqs (17) and (22) the maximum attenuation results then as

$$(\alpha_{HE})_{\max} = \frac{m}{\beta_0 a^2 \left[1 - \left(\frac{m}{\sigma_{mn}} \right)^2 \right]}, \quad m, n = 1, 2, 3, \text{ etc.} \quad (46)$$

Equation (46) shows that the maximum attenuation is inversely proportional to the square of the inner radius of the ring-element guide and inversely proportional to frequency. The higher thus the frequency, the lower the maximum attenuation. Neglecting the term $(m/\sigma_{mn})^2$ the maximum attenuation is proportional to m ($m=1,2,3$, etc.). It should here be noted that the material constants of the outer medium do not appear in eq (46). Since with the eqs (42) to (44) ϵ_i was assumed as real and the losses due to the rings were not taken into account, the inequality (41) must, of course, always be satisfied.

Equation (44) shows that always only for *one* σ_{mn} , i.e., for one mode, the conditions for maximum attenuation can be satisfied. The condition eq (44) can be interpreted as kind of a matching condition.

An example may show the application of eqs (42) to (46). Let us assume that a ring-element guide is to be found with maximum attenuation of the HE_{12} -mode. This mode is excited with particular ease by the H_{01} -mode in a homogeneous waveguide whenever it deviates from its straight circular shape and it has a relatively low attenuation.

Given are the following data: Frequency $f = 50$ kMc/s ($\lambda_0 = 6$ mm); $a = 2.5$ cm, hence $\beta_0 a = 26.2$. With the HE_{12} -mode there is $\sigma_{mn} = \sigma_{12} = 5.33$. From eq (46) there results then the maximum attenuation of the HE_{12} -mode as $\alpha_{12} = 0.0158$ N/cm, i.e., 3,180 times the attenuation

in the homogeneous circular copper waveguide. It is further assumed that a dielectric with $\epsilon/\epsilon_0=10(1-j)$ and $\mu=\mu_0$ is available for constructing the ring-element guide. The attenuation of the fields in the outer medium is then $\text{Im}(\beta_0 \sqrt{\epsilon/\epsilon_0})=15 \text{ N/cm}$. Besides it is assumed that $D_2=D_1$. Find now the quantities ϵ_i/ϵ_0 and d .

With the given values there results from the eqs (42) to (45): $U=0.242$; $V=0.093$; $R=0.553$; $Z_B/Z_0=0.344$; $\tan(\beta_0 \sqrt{\epsilon_i/\epsilon_0} d)=2.08$, i.e., $\epsilon_i/\epsilon_0=2.11$; $d=0.74 \text{ mm}$. Because of $D_2=D_1$ the attenuation of the HE_{01} -mode, according to eq (31) in this case exceeds that in the homogeneous waveguide by the factor $\sqrt{2}$.

While in the above example the increase in attenuation over the homogeneous waveguide is very high with the HE_{12} -mode, this holds no longer for the other HE_{1n} -modes. If, however, maximum attenuation of a specific mode is no longer demanded, an appropriate dimensioning of the ring-element guide allows a design that the attenuation values of a number of HE_{mn} -mode approach more closely their maximums.

Another interesting point is the basic attenuation/frequency curve of a HE_{mn} -mode. For the dimensions calculated in the example, the figure 7 shows the attenuation of the HE_{12} -mode as a function of $\sqrt{\epsilon_i/\epsilon_0} d/\lambda_0$ with a fixed $\sqrt{\epsilon_i/\epsilon_0} d$, i.e., as a function of frequency. Here, however, there must be $D_1=D_2<0.2 \text{ mm}$, to have inequality (1) satisfied for all frequencies stated in figure 7. With the maximum attenuation attainable the curve plotted in figure 7 presents a pointed peak at $\sqrt{\epsilon_i/\epsilon_0} d/\lambda_0=0.179$ ($f=50 \text{ kMc/s}$). The other extremities of the curve are no such peaks, but ordinary maximums. They are all lower than this peak, since according to eq (22) $\beta_0 a$ and thus the frequency is in the denominator of the attenuation constant. On the frequency axis the first maximum is away from the peak by 0.25. The subsequent maximums are spaced 0.5 from each other. Since the losses of the rings were neglected, the attenuation at the cutoff frequency is here zero.

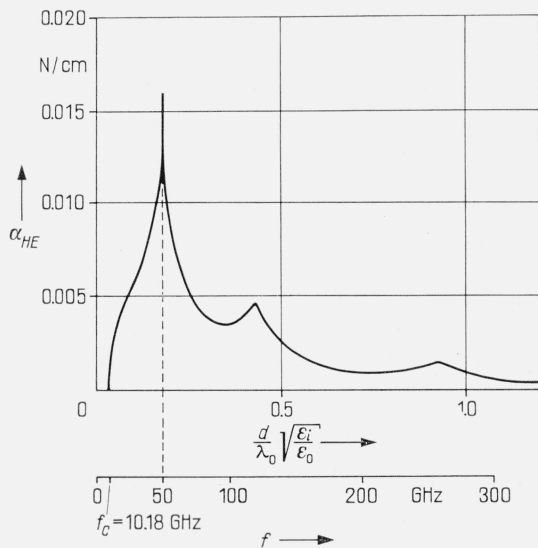


FIGURE 7. Attenuation of the HE_{12} -mode as a function of frequency with a ring-element guide with $\epsilon_i/\epsilon_0=10(1-j)$, $\mu=\mu_0$, $\epsilon_i/\epsilon_0=2.11$, $d=0.74 \text{ mm}$, $a=2.5 \text{ cm}$, $D_1=D_2$.

At this point let us also make some statements concerning the capability of existence of the waveguide modes. If the outer medium and the dielectric between the rings are free of losses, the quantity Z_a/Z_0 is in the left half-plane of the complex number plane when the ring losses are neglected, according to eq (27). Only with a consideration of the ring losses and a very large thickness d the quantity Z_a/Z_0 lies in the right-hand half of the complex number plane, so that $\text{Re}(Z_a/Z_0)>0$, and a sufficient condition is so satisfied for the capability of existence of waveguide modes.

4.3. Properties of the EH_m -Modes

a. General Considerations

The term EH_m -modes ($m=0, 1, 2$, etc.) is understood herein as comprising modes of E -character whose fields disappear in the region $0 \leq r \leq a$ in the axis ($r=0$) or at the point $r=a$ at most (the Bessel functions have then no zeros in $0 < r < a$). For $r > b$ the fields disappear only in the infinite. The subscript n therefore can be dropped with these modes. The surface modes, i.e., modes most of whose fields are outside the guide, hence in the region $r > b$, are counted as a rule as EH_m -modes. As will be shown below, the surface modes with H -character have no practical significance because of their high attenuation. As a rule the phase velocity of the EH_m -modes is less than the velocity of light. With the EH_m -modes the ring-element guide thus is, as a rule, a delay line. The principal characteristics of the EH_m -modes are obvious already from the special case of the rotation-symmetrical modes ($m=0$). Let us thus consider above all these modes. With

$$\left. \begin{array}{l} |p_E a| \\ |k_0 a| \\ |k_2 b| \\ |\beta_2 b| = \beta_0 b \sqrt{\frac{\mu \epsilon}{\mu_0 \epsilon_0}} \end{array} \right\} \gg 1, \quad (47)$$

$$\text{Im}(k_0 a) > 2 \quad (48)$$

there results from eq (87)

$$\frac{k_0}{\beta_0} = \frac{Z_a}{Z_0} = \frac{Z_A}{Z_0} \frac{1 + j \frac{Z_E}{Z_A} \tan p_E d}{1 + j \frac{Z_A}{Z_E} \tan p_E d}, \quad \text{for } m=0. \quad (49)$$

Insertion of eq (29) into eq (49) and resolution for $\tan p_E d$ yields

$$\tan p_E d = -j \frac{\frac{k_0}{\beta_0} \frac{\epsilon}{\epsilon_0} \pm \sqrt{\left(\frac{\mu \epsilon}{\mu_0 \epsilon_0} - 1\right) + \left(\frac{k_0}{\beta_0}\right)^2}}{\frac{Z_E}{Z_0} \frac{\epsilon}{\epsilon_0} \pm \frac{Z_0}{Z_E} \frac{k_0}{\beta_0} \sqrt{\left(\frac{\mu \epsilon}{\mu_0 \epsilon_0} - 1\right) + \left(\frac{k_0}{\beta_0}\right)^2}} \quad \text{for } m=0. \quad (50)$$

The root in eq (50) is k_2/β_0 . If $|\text{Im}((k_0/\beta_0)^2)| > |\text{Im}(\mu\epsilon/(\mu_0\epsilon_0))|$ the upper sign of eq (50) holds. If, however, $|\text{Im}((k_0/\beta_0)^2)| < |\text{Im}(\mu\epsilon/(\mu_0\epsilon_0))|$ the lower sign holds in eq (50).

With

$$\left. \begin{array}{l} \left| \frac{m}{k_0 a} \right| \\ \left| \frac{4m^2}{(\beta_0 a)^2} \left[\left(\frac{\beta_0 a}{k_0 a} \right)^2 - 1 \right] \right| \end{array} \right\} \ll 1 \quad m=1,2,3,\dots \quad (51)$$

equation (50) holds approximately also for $m \neq 0$. With use of eq (50) it should always be borne in mind, however, that the inequality (47) must be satisfied.

Because of the losses of the guide the eigenvalue $k_0 a$ is complex and there is set accordingly

$$\frac{k_0}{\beta_0} = \xi + j\eta. \quad (52)$$

The quantity k_0/β_0 is imaginary, i.e.,

$$\frac{k_0}{\beta_0} = j\eta \quad (53)$$

and there holds the upper sign in eq (50). The quantity k_0/β_0 must also be imaginary, i.e.

$$\left| \left(\frac{k_0}{\beta_0} \right)^2 \right| > \frac{\mu\epsilon}{\mu_0\epsilon_0} - 1. \quad (54)$$

For a real $\mu\epsilon/(\mu_0\epsilon_0) \neq 1$ the ring-element guide is a delay line with a periodic band pass character, because of the imaginary k_0/β_0 and the condition of the inequality (54). Apart from the H_{0n} -modes no wave guide modes are capable of existence. The limit of the pass band and stop band of the delay line is found from eq (54) with $|(k_0/\beta_0)^2| = \mu\epsilon/(\mu_0\epsilon_0) - 1$ and lies at

$$\left(\frac{2\pi}{\lambda_0} \sqrt{\frac{\epsilon_i}{\epsilon_0}} d \right)_g = \arctan \frac{Z_0}{Z_E} \sqrt{\frac{\mu\epsilon}{\mu_0\epsilon_0} - 1}. \quad (55)$$

For $\mu\epsilon \rightarrow \infty$ there is $\sqrt{\epsilon_i/\epsilon_0} d/\lambda_0 = 0.25 + \nu 0.5$; $\nu = 0, 1, 2$, etc.

In the special case $\mu\epsilon/(\mu_0\epsilon_0) = 1$ there is $k_2 = k_0$ and eq (50) yields

$$\frac{k_0}{\beta_0} = j \frac{Z_E}{Z_0} \tan \left(\frac{\pi}{\lambda_0} \sqrt{\frac{\epsilon_i}{\epsilon_0}} d - \begin{cases} 0 \\ \frac{\pi}{2} \end{cases} \right). \quad (56)$$

Also in this case the ring-element guide is a delay line, but without band pass character.

As an example, figure 8 shows the relative eigenvalue η with the E_0 -mode as a function of $\sqrt{\epsilon_i/\epsilon_0} d/\lambda_0$ for $\mu = \mu_0$, but different ϵ_i and ϵ . Figure 8 is to be thought of as continued periodically in the direction of increasing $\sqrt{\epsilon_i/\epsilon_0} d/\lambda_0$, the period amounting to 0.5. The mode will travel the slower, the higher the dielectric constant of the outer medium and the closer Z_E approaches Z_0 , i.e., if D_2/D_1 is small. With a high D_2/D_1 , e.g., for $D_2/D_1 = 5$, the relative eigenvalue at the beginning of the pass band is almost independent of d/λ_0 , but increases the more steeply later on.

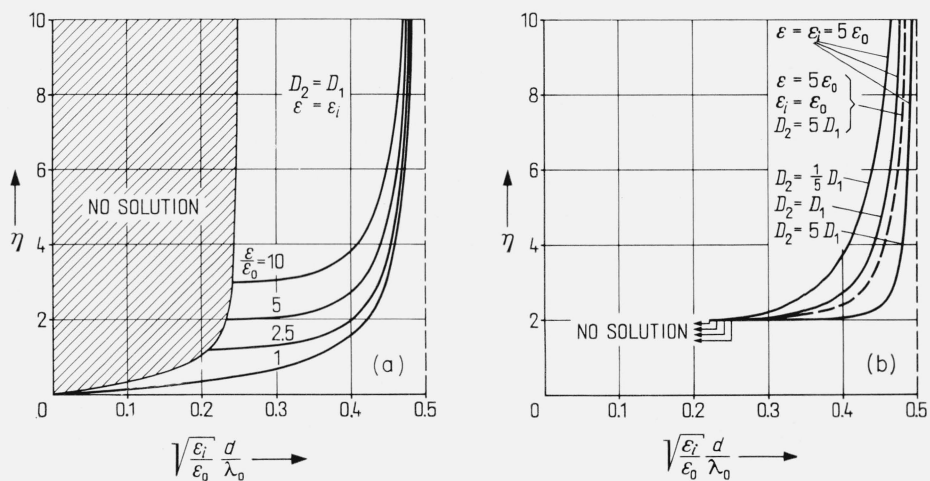


FIGURE 8. The relative eigenvalue $k_0/\beta_0 = j\eta$ with the E_0 -mode in the ring-element guide as a function of $\sqrt{\epsilon_i/\epsilon_0} d/\lambda_0$ for various ϵ, ϵ_i and D_2/D_1 .

The presentation is to be thought of as periodically continued with the period 0.5 in the direction of increasing $\sqrt{\epsilon_i/\epsilon_0} d/\lambda_0$.

For the special case $d=0$ there results from eq (50)

$$\frac{k_0}{\beta_0} = j \sqrt{\frac{\frac{\mu\epsilon}{\mu_0\epsilon_0} - 1}{\left(\frac{\epsilon}{\epsilon_0}\right)^2 - 1}} \quad (57)$$

It should here be noted that the inequality (48) must always be satisfied and k_0 must have a positive real and imaginary part. With a real ϵ the eq (57) thus yields no solution even if μ complex. From the propagation constant γ there results with $|k_0^2| \gg \beta_0^2$ in the case $d=0$ a maximum attenuation for $\tan \delta = 1 + \epsilon_0/\epsilon_a$, if $\epsilon/\epsilon_0 = \epsilon_a/\epsilon_0(1 - j \tan \delta)$.

In the special case $\sqrt{\epsilon_i/\epsilon_0}d/\lambda_0 = 0.25$ eq (50) yields

$$\frac{k_0}{\beta_0} = j \sqrt{\frac{1}{2} \left(\frac{\mu\epsilon}{\mu_0\epsilon_0} - 1 \right) + \sqrt{\frac{1}{4} \left(\frac{\mu\epsilon}{\mu_0\epsilon_0} - 1 \right)^2 + \left(\frac{Z_E}{Z_0} \right)^4 \left(\frac{\epsilon}{\epsilon_0} \right)^2}} \quad (58)$$

Unlike eq (57) the eq (58) holds for real $\mu\epsilon/(\mu_0\epsilon_0)$ as well.

Setting $\mu = \mu_a(1 - j \tan \delta_\mu)$ and $\epsilon = \epsilon_a(1 - j \tan \delta_\epsilon)$, and if the outer medium has but small losses, there holds $\tan \delta_\mu + \tan \delta_\epsilon \ll 1$. In such case the imaginary part of the eigenvalue, i.e., η of eq (52) practically agrees with the solution for a real $\mu\epsilon$. Figure 9 shows under these assumptions for $\mu = \mu_0$ and $\tan \delta_\epsilon = \tan \delta$ the quantity $\xi/\tan \delta$ as a function of $\sqrt{\epsilon_i/\epsilon_0}d/\lambda_0$ with the E_0 -mode. The dielectric constant ϵ_i and the real part of ϵ agree with figure 8. The quantity η can be taken from figure 8. A comparison with this diagram shows that with an increasing η the quantity ξ increases correspondingly. The periodic band pass character has been retained.

If the outer medium is very lossy, the real part of the eigenvalue and accordingly the quantity ξ will be larger than in figure 9. As an example the figure 10 shows the relative eigenvalue k_0/β_0 with the E_0 -mode as a function of d/λ_0 for $\epsilon_i = \epsilon_0$ and $\epsilon/\epsilon_0 = 5; 5(1 - j 0.3); 5(1 - j)$. The periodic band pass character remains also in this case, but in the pass bands there exist as a rule for each d/λ_0 two different eigenvalues which are plotted in the figures 10a and 10b. Only with a real ϵ there results only one eigenvalue for each d/λ_0 . According to figure 8 it is imaginary, and therefore it is on the imaginary axis in figure 10b. In figure 10a there is $|k_0| < \beta_0$ and in figure 10b $|k_0| > \beta_0$.

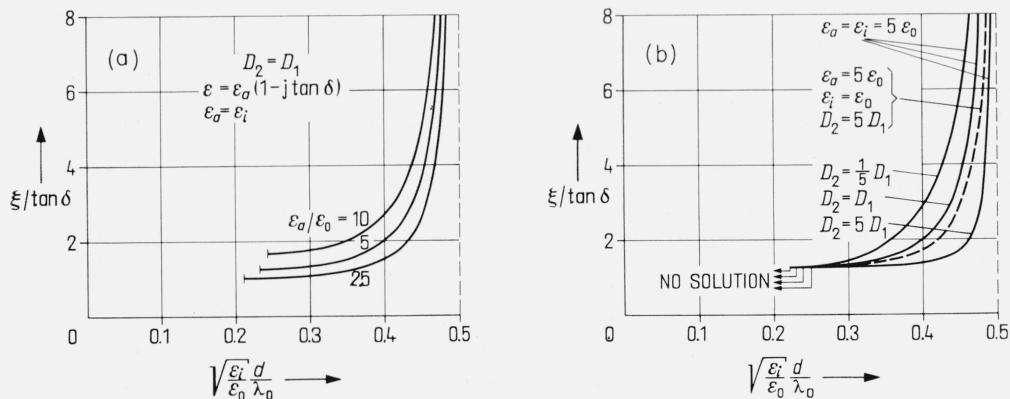


FIGURE 9. The real part ξ of the relative eigenvalue $k_0/\beta_0 = \xi + j\eta$ with the E_0 -mode in the ring-element guide as a function of $\sqrt{\epsilon_i/\epsilon_0}d/\lambda_0$ for various ϵ , ϵ_i , and D_2/D_1 under the assumption $\tan \delta \ll 1$ (δ loss angle of the dielectric outside the rings).

Because of $\tan \delta \ll 1$ η is to be taken from figure 8. The presentation is to be thought of as periodically continued with the period 0.5 in the direction of increasing $\sqrt{\epsilon_i/\epsilon_0}d/\lambda_0$.

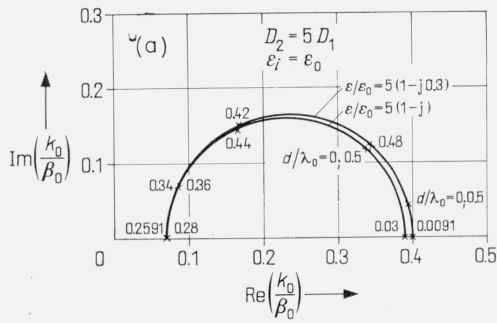
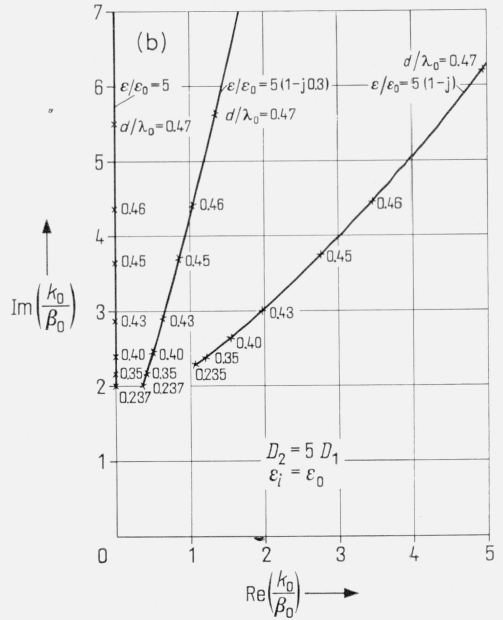


FIGURE 10. The relative eigenvalue k_0/β_0 with the E_0 -mode in the ring-element guide as a function of d/λ_0 for $\epsilon_i = \epsilon_0$, $D_2 = 5D_1$ and various ϵ .



The eigenvalue in figure 10b corresponds to that in figure 8. The pass bands of figures 10a and 10b differ slightly. With $\epsilon/\epsilon_0 = 5(1-j)$ for example, the pass band is given in figure 10a by $0 < d/\lambda_0 < 0.03$ and $0.28 < d/\lambda_0 < 0.5$. In figure 10b the pass band is given in this case by $0.235 < d/\lambda_0 < 0.5$. In either case the pass bands recur with the period $d/\lambda_0 = 0.5$.

The solution in figure 10a is very easily found, since the quantity k_0^2 can here be neglected with respect to $\beta_0^2(\mu\epsilon/(\mu_0\epsilon_0) - 1)$. The relative eigenvalues k_0/β_0 lie therefore on a circle of which only the part in the first quadrant of the complex number plane ($\text{Im}(k_0) > 0$) gives a physically reasonable solution.

The solution in figure 10b is more difficult to find (see [7]). With $\epsilon/\epsilon_0 = 5(1-j0.3)$ the solution in figure 10b practically agrees with the values η and ξ resulting from the dashed curves of the figures 8b and 9b.

Besides the EH_m -modes and the H_{0n} -modes which are always capable of existence, even waveguide modes can propagate, if the inequality (41) holds (see sec. 4.1 and 4.2).

4.4. Special Case $a=0$, E_0 -Mode

For $a \rightarrow 0$ the ring-element guide changes into the guide discussed in [10] (fig. 11, in [10] there has indeed been assumed $\mu = \mu_0$ and $\epsilon = \epsilon_0$). With this guide most of the wave energy travels outside indeed, hence in the region $r > b$, and these modes thus are typical surface modes. The quantity k_2 and thus the propagation constants of these modes are obtained from equation (89). There results that with an outer medium consisting of a dielectric (in particular with $\epsilon = \epsilon_0$ and $\mu = \mu_0$) only the E_0 -mode is of practical interest. The H_0 , HE_{mn} , and EH_m -modes ($m \neq 0$) have very high attenuation and correspond to the spurious modes on the Sommerfeld guide. Compare hereto also the statements in [9].

For the E_0 -mode one obtains with $\beta_2 = \beta_0 \sqrt{\mu\epsilon/(\mu_0\epsilon_0)}$ from the eq (89) to (92) for the calculation of k_2

$$\frac{\beta_2 H_1^{(1)}(k_2 b)}{k_2 H_0^{(1)}(k_2 b)} = \sqrt{\frac{\mu\epsilon_i}{\mu_0\epsilon}} \frac{D_1 + D_2}{D_1} \frac{J_1(p_E b)}{J_0(p_E b)} \quad (59)$$

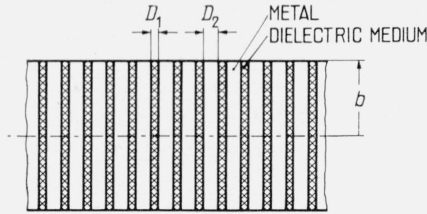


FIGURE 11. Ring-element guide with $a=0$.

Also the ring-element guide with $a=0$ has practically a periodic band pass character. Since k_2 always must have a positive imaginary part, there result from eq (59) with the lossless guide the stop bands:

$$\chi_{0n} < \beta_0 \sqrt{\frac{\epsilon_i}{\epsilon_0}} b < \sigma_{0n}, \quad (60)$$

and pass bands:

$$\sigma_{0n} < \beta_0 \sqrt{\frac{\epsilon_i}{\epsilon_0}} b < \chi_{0(n+1)} \quad n=1, 2, 3, \text{ etc.}$$

For $\epsilon=\epsilon_0$ and $\mu=\mu_0$ the eqs (59) and (60) have been stated already in [10].

With

$$\left. \begin{array}{l} |k_2 b| \\ |p_E b| \end{array} \right\} \gg 1 \quad (61)$$

one obtains from eq (59)

$$\frac{k_2}{\beta_2} = j \sqrt{\frac{\mu_0 \epsilon}{\mu \epsilon_i}} \frac{D_1}{D_1 + D_2} \tan \left(p_E b + \frac{\pi}{4} \right). \quad (62)$$

Without consideration of the losses there are then the stop bands:

$$n\pi - \frac{\pi}{4} < \beta_0 \sqrt{\frac{\epsilon_i}{\epsilon_0}} b < n\pi + \frac{\pi}{4} \quad (63)$$

and the pass bands:

$$n\pi + \frac{\pi}{4} < \beta_0 \sqrt{\frac{\epsilon_i}{\epsilon_0}} b < (n+1)\pi - \frac{\pi}{4} \quad n=1, 2, 3, \text{ etc.}$$

A comparison between the inequalities (60) and (63) shows that the inequality (63) is sufficiently accurate for practical purposes.

After inserting eq (62) into eq (12) one obtains with

$$\frac{\epsilon_i}{\epsilon_0} = \frac{\epsilon_{i1}}{\epsilon_0} (1 - j \tan \delta_i), \quad (64)$$

$$\tan \delta_i \ll 1, \quad (65)$$

$$\beta_1 b = \beta_0 \sqrt{\frac{\epsilon_{i1}}{\epsilon_0}} b, \quad (66)$$

$$|\operatorname{Re}(k_2)| \ll |\operatorname{Im}(k_2)| \quad (67)$$

for the phase and attenuation constants with $\epsilon=\epsilon_0$ and $\mu=\mu_0$

$$\beta = \beta_0 \sqrt{1 + \left[\sqrt{\frac{\epsilon_0}{\epsilon_{i1}}} \frac{D_1}{D_1 + D_2} \tan \left(\beta_1 b + \frac{\pi}{4} \right) \right]^2} \quad (68)$$

$$\alpha = \beta_0 b \frac{D_1}{D_1 + D_2} \frac{\frac{\beta_0}{2} \tan \delta_i + \frac{1}{D_1} \sqrt{\frac{\beta_0}{2Z_{0K}}}}{\cos^2 \left(\beta_1 b + \frac{\pi}{4} \right) \sqrt{1 + \left[\sqrt{\frac{\epsilon_{i1}}{\epsilon_0}} \frac{D_1 + D_2}{D_1} \cot \left(\beta_1 b + \frac{\pi}{4} \right) \right]^2}} \quad (69)$$

The eq (68) shows that the phase velocity of the E_0 -mode as a rule is less than the velocity of light. In eq (69) the minute losses of the metal at the surface of the guide, i.e., for $r=b$ have been neglected. The attenuation-versus-frequency response is analogous to the one shown in figure 8 of [9]. Compare hereto also [10].

If

$$|\operatorname{Im}(p_E b)| > 2 \quad (70)$$

with $\epsilon = \epsilon_0$ and $\mu = \mu_0$ eq (62) can be written as the simple formula

$$\frac{k_2}{\beta_2} = \frac{k_0}{\beta_0} = \sqrt{\frac{\epsilon_0}{\epsilon_i}} \frac{D_1}{D_1 + D_2} = \frac{Z_E}{Z_0} \quad (71)$$

Equation (71) yields the special case that, under the condition of the inequality (70), the E_0 -mode as a surface mode has a phase velocity higher than the velocity of light. See hereto also the examples at the end of section 5.

5. Disk Guide (Ring-Element Guide With $d = \infty$)

For calculating the propagation constants of the modes in the disk guide (fig. 1) the formulas for the ring-element guide are used, replacing Z_a/Z_0 by Z_E/Z_0 . With the waveguide modes the eqs (13) to (40) hold accordingly, i.e., the H_{0n} -modes have the same attenuation as with the ring-element guide. With the E_{0n} -modes there is under the assumption

$$\left| \frac{Z_E}{Z_0} \right| < \frac{\chi_{0n}}{\beta_0 a} \quad n=1,2,3, \text{ etc.} \quad (72)$$

the attenuation

$$\alpha_E = \frac{1}{a \sqrt{1 - \left(\frac{\chi_{0n}}{\beta_0 a} \right)^2}} \operatorname{Re} \left(\frac{Z_E}{Z_0} \right) \quad n=1,2,3, \text{ etc.} \quad (73)$$

The phase constant practically equals that in the lossless homogeneous waveguide.

Corresponding to the eqs (48) and (49) there appears under the assumption

$$\operatorname{Im} \left(\frac{Z_E}{Z_0} \right) > \frac{2}{\beta_0 a} \quad (74)$$

the equation

$$\frac{k_0}{\beta_0} = \frac{Z_E}{Z_0} \quad (75)$$

Because of the inequality (74) the Bessel functions have no zeros in $0 < r < a$ and the subscript n is therefore not needed. The E_{0n} -mode has changed into an E_0 -mode. Note that eq (75) agrees with eq (71). With

$$\left| \frac{Z_E}{Z_0} \right| >> \frac{1}{\beta_0 a} \quad (76)$$

there is then

$$\gamma = \pm j \beta_0 \sqrt{1 - \left(\frac{Z_E}{Z_0} \right)^2} \quad (77)$$

Some examples are to show the applications of the eqs (73) and (77) for the E_{01} -mode and E_0 -mode. There is $\chi_{01} = \chi_{01} = 2.41$. The frequency is always assumed as $f = 50$ kMc/s, hence $\lambda_0 = 0.6$ cm and the inner radius is $a = 2.5$ cm.

For $D_2 = 50 D_1$ and $\epsilon_i/\epsilon_0 = 3$ the inequality (72) is satisfied and there results from eq (73) the attenuation $\alpha_E = 4.54 \times 10^{-3}$ N/cm. This attenuation comes about merely by radiation into the inhomogeneous medium and is 72.5 times larger than the attenuation of the E_{01} -mode in the homogeneous circular copper waveguide.

For $D_2=50 D_1$ and $\epsilon_i/\epsilon_0=3(1-j)$ the eq (72) can be used as well and there results $\alpha_E=3.52 \times 10^{-3}$ N/cm. Despite the lossy dielectric the attenuation is now lower, since Z_E deviates from Z_0 more heavily than with $\epsilon_i/\epsilon_0=3$ (poorer matching of the radial impedance).

With $D_2=D_1$ and $\epsilon_i/\epsilon_0=3(1-j)$ the inequalities (74) and (76) are satisfied and there results from eq (77) an attenuation $\alpha_E=0.223$ N/cm, i.e., 3.55×10^3 times as much as the attenuation of the E_{01} -mode in the homogeneous circular copper waveguide. The phase constant is 1.8 percent less than that in the homogeneous waveguide. Compared to the case $D_2=50 D_1$ the propagation constant thus has changed much more strongly relative to that in the homogeneous waveguide. In particular the attenuation has increased very heavily (superior matching of Z_E to Z_0).

With $D_2=D_1$ and $\epsilon_i/\epsilon_0=2.5(1-j)$ there results then an even higher attenuation, i.e., $\alpha_E=0.269$ N/cm, since Z_E has approached Z_0 even more. In this case the phase constant is 2.1 percent less than that in the homogeneous waveguide.

With the examples for the E_0 -mode the fact is remarkable that the phase velocity is not only greater than the velocity of light, but also greater than the phase velocity of the E_{01} -mode in the homogeneous waveguide. This is in contrast to the general behavior of the E_0 -mode which is characterized by $v_p < c$ (see notes in sec. 4).

6. Disk Loaded Waveguide and the Corrugated Waveguide (Ring-Element Guide With $\epsilon = \kappa/j\omega$ and $\mu = \mu_0$). E_{0n} -mode and E_0 -mode with $\epsilon_i = \epsilon_0$ and $\kappa = \infty$

The eigenvalues for the modes in the disk-loaded waveguide and corrugated waveguide are obtained from the eqs (83) and (84) by setting $\epsilon = \kappa/j\omega$ and $\mu = \mu_0$. All formulas derived in discussing the ring-element guide can thus here be used as well. To bring out clearly the fundamentals of the disk loaded waveguide and the corrugated waveguide, let us here consider merely the E_{0n} and E_0 -modes with $\epsilon_i = \epsilon_0$, neglecting the losses ($\kappa = \infty$).

As a first step there results quite generally that for $\beta_0 b \ll 1$ no propagating modes exist in the disk loaded waveguide and corrugated waveguide, but merely statically attenuated fields of the type of the waveguide fields.

With $\beta_0 a \ll 1$ and $\beta_0 b \gg 1$, however, the disk loaded waveguide is a delay line with filter character and very narrow pass bands. For the E_0 -mode there result the eigenvalues $k_0 a$ and the pass bands from

$$k_0 a \frac{J_0(k_0 a)}{J_1(k_0 a)} = (\beta_0 a)^2 \frac{D_1}{D_1 + D_2} \frac{\pi}{2} \frac{1}{\beta_0 b - \frac{\pi}{4} - k \frac{\pi}{2}} \geq 2 \quad k=1,3,5, \text{ etc } \dots \quad (78)$$

The pass bands are given accordingly by

$$k \frac{\pi}{2} + \frac{\pi}{4} \leq \beta_0 b \leq k \frac{\pi}{2} + \frac{\pi}{4} + (\beta_0 a)^2 \frac{D_1}{D_1 + D_2} \frac{\pi}{4} \quad k=1,3,5, \text{ etc.} \quad (79)$$

Particularly interesting is the behavior of the line with $\beta_0 a \gg 1$. This case shall be considered alone hereinafter. The eigenvalues $k_0 a$ are now obtained from

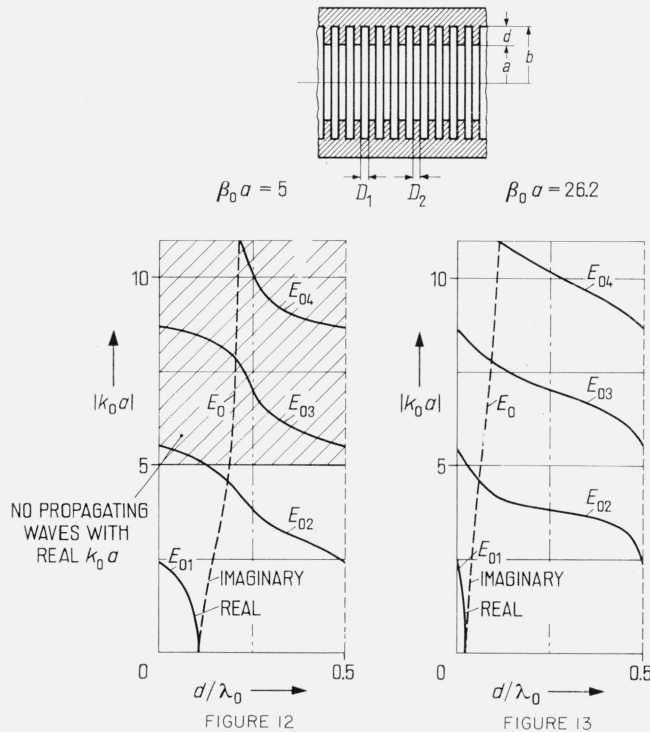
$$k_0 a \frac{J_0(k_0 a)}{J_1(k_0 a)} = \beta_0 a \frac{D_1}{D_1 + D_2} \tan \beta_0 d. \quad (80)$$

With $d=0$, the solutions of eq (80) are the zeros of $J_0(k_0 a)$. There result the E_{0n} -modes for the homogeneous waveguide.

With $d/\lambda_0=0.25$ the solutions of eq (80) are the zeros of $J_1'(k_0 a)$ and the $E_{0(n+1)}$ -modes have the same phase velocity as the H_{0n} -modes. (The notation $E_{0(n+1)}$ derives from the fact that with $d \rightarrow 0$ the waveguide mode $E_{0(n+1)}$ comes about, see also figs. 12 and 13.) Physically, this can be explained as follows. With $d/\lambda_0=0.25$ the input impedance for $r=a$ is infinite for a mode in the radial direction. This means that no current flows at this point and $H_\varphi=0$ accord-

ingly. Since, however, with the E -modes H_ϕ follows the same function as E_ϕ with the H -modes, and since with these the field strength $E_\phi=0$ for $r=a$, the same phase constant results with $d/\lambda_0=0.25$ for the $E_{0(n+1)}$ -modes as for the H_{0n} -modes. The figures 12 to 15 show a further evaluation of eq (80).

The figures 12 and 13 present the eigenvalues k_0a of the E_{0n} -modes and the E_0 -mode as a function of d for a given β_0a , i.e., for a given frequency. The figures 12 and 13 must be thought of as periodically continued in the direction of increasing d/λ_0 with the period 0.5, corresponding to the period of $\tan \beta_0d$. With $d=0$ one obtains the solutions for the homogeneous waveguide. With increasing d the real k_0a decreases with the E_{0n} -modes and the imaginary k_0a increases with the E_0 -mode, i.e., the mode travels the slower, the higher d .



FIGURES 12 and 13. The eigenvalues k_0a with the E_{0n} -modes ($n=1,2,3,4$) and with the E_0 -mode (k_0a imaginary) in the disk loaded waveguide as a function of d for $D_2=D_1$ and fixed β_0a .

The presentation is to be thought of as periodically continued with the period 0.5 in the direction of increasing d/λ_0 .

As an example let us once more consider figure 12. All values $k_0a > \beta_0a = 5$ give no propagating modes, only statically attenuated fields. This is shown in figure 12 by cross-hatching.

Let us now study more closely the curve marked E_{01} . For $d=0$ there results $k_0a=2.4$, i.e., the eigenvalue of the E_{01} -mode in the homogeneous waveguide. With increasing d the quantity k_0a decreases (the mode travels more slowly) to reach finally zero for $d/\lambda_0=0.11$. The phase velocity of the mode now equals the velocity of light. The curve marked E_{01} can now be thought of as continued by the curve marked E_0 , i.e., the more d increases, the more the E_{01} -mode changes into the E_0 -mode whose phase velocity is less than the velocity of light. The guide now is for this mode a delay line, the eigenvalue k_0a is imaginary and increases with increasing d . With $d/\lambda_0=0.25$ the quantity $k_0a=j\infty$. In the range $0.25 < d/\lambda_0 < 0.5$ no E_{01} -mode and no E_0 -mode are present. For $d/\lambda_0 > 0.5$ this repeats itself periodically with the period 0.5.

Let us now study closely the curve marked E_{02} . With $d=0$ there results $k_0a=5.52$, i.e., the eigenvalue for the E_{02} -mode in the homogeneous waveguide. With $k_0a > \beta_0a$ no propagating mode is possible, however. With increasing d the quantity k_0a decreases to attain finally the value 5 for $d/\lambda_0=0.12$ so that a propagating mode exists for $d/\lambda_0 > 0.12$. For $d/\lambda_0=0.25$ the quantity k_0a is $=3.83$. The E_{02} -mode now has the same phase velocity as the H_{01} -mode. With a further increase of d the quantity k_0a finally changes for $d/\lambda_0=0.5$ into the eigenvalue of the E_{01} -mode in the homogeneous waveguide, i.e., $k_0a=2.4$. For $d/\lambda_0 > 0.5$ it is the E_{01} -curve shifted by $d/\lambda_0=0.5$ in a horizontal direction that continues the curve.

The curve marked E_{03} is of a similar shape; for $d=0$ there results from it the eigenvalue 8.65 of the E_{03} -mode, for $d/\lambda_0=0.5$ the eigenvalues 5.52 of the E_{02} -mode, and for $d/\lambda_0=1$ the eigenvalue 2.4 of the E_{01} -mode in the homogeneous waveguide. For $0.5 < d/\lambda_0 < 1$ the curve E_{02} shifted horizontally by $d/\lambda_0=0.5$ thus continues the curve. For $d/\lambda_0 > 1$ there follows subsequently the E_{01} -curve shifted by $d/\lambda_0=1$. The curve E_{04} , etc. runs correspondingly, and so on.

Fig. 13 shows the behavior of the guide for $\beta_0 a = 26.2$. Because of the large $\beta_0 a$, the E_{03} and E_{04} -modes are here capable of existence, in contrast to figure 12. Besides the E_{01} -mode changes into the E_0 -mode already for $d/\lambda_0 = 0.025$. With a waveguide radius $a = 2.5$ cm a delay line thus comes about already for $d > 0.15$ mm. Such a depth of $d = 0.15$ mm may result already by circular furrows due to roughing.

The figures 14 and 15 show the eigenvalues $k_0 a$ of the E_{0n} -modes and of the E_0 -mode as a function of the frequency (d/λ_0). The associated $\beta_0 a$ is also shown for each frequency. This gives a straight line through the origin. The higher the slope of this line, the smaller the ratio d/a (see the figs. 14 and 15). Above this straight line the real eigenvalues $k_0 a$ are greater than $\beta_0 a$ so that no propagating modes with real $k_0 a$ are here possible. The curves do not hold for any desired small values d/λ_0 , for the condition $\beta_0 a \gg 1$ is then no longer satisfied. Since $\beta_0 a$ here is a function of d/λ_0 , the figures 14 and 15 are no longer periodical, unlike the figures 12 and 13. This is most distinct with the values $k_0 a = 0$. The higher d/λ_0 , the more these values lie at $d/\lambda_0 = p \cdot 0.5$ ($p = 1, 2, 3$, etc.).

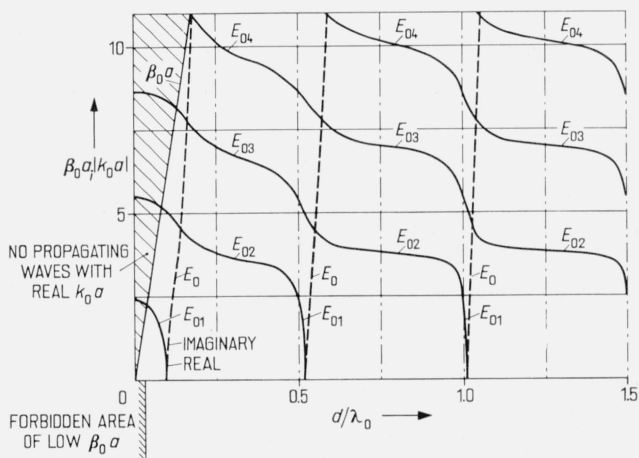
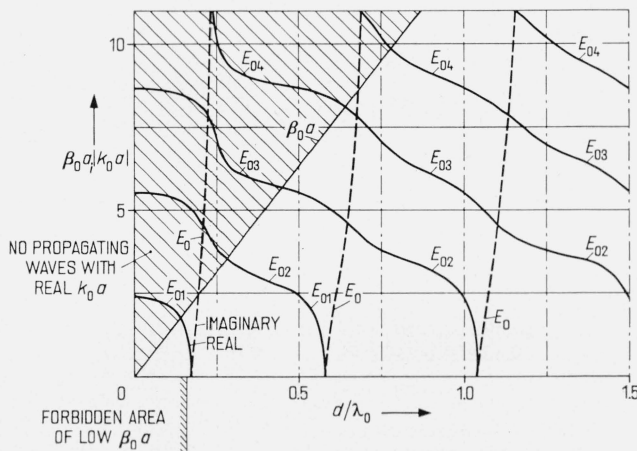


FIGURE 14. The eigenvalues $k_0 a$ with the E_{0n} -modes ($n=1,2,3,4$) and with the E_0 -mode ($k_0 a$ imaginary) in the disk loaded waveguide as a function of the frequency (d/λ_0) in the range $0.03 < d/\lambda_0 \leq 1.5$.

Here $D_2 = D_1$; $d = a/10$; $a = 2.5$ cm.

FIGURE 15. The eigenvalues $k_0 a$ with the E_{0n} -modes ($n=1,2,3,4$) and with the E_0 -mode ($k_0 a$ imaginary) in the disk loaded waveguide as a function of the frequency (d/λ_0) in the range $0.16 < d/\lambda_0 \leq 1.5$.

Here $D_2 = D_1$; $d = a/2$; $a = 2.5$ cm.



If we consider the range of validity of the curves in the figures 14 and 15, it is evident that d/λ_0 can always be so chosen that only *one* E_{0n} -mode is capable of existence. For example, in figure 14 ($d=a/10$) only the E_{01} -mode is capable of existence with $d/\lambda_0=0.08$. In figure 15 ($d=a/2$) only the E_{02} -mode is capable of existence for $0.28 < d/\lambda_0 < 0.45$.

If d/λ_0 is so chosen that the E_0 -mode is capable of existence, the ranges of validity of the figures 14 and 15 yield that in addition at least the E_{02} -mode is capable of propagation. This holds, for instance in figure 14, for the range $0.095 < d/\lambda_0 < 0.13$ and in figure 15 for $0.58 < d/\lambda_0 < 0.64$. For larger d/λ_0 the E_{03} -mode comes to these as well.

The figures 16 to 21 show in the region $0 \leq r \leq a$ the field configurations of the modes capable of existence at $\beta_0 a = 5$, $a = 2.5$ cm ($\lambda_0 = \pi$ cm), $D_2 = D_1$ for a number of d/λ_0 .

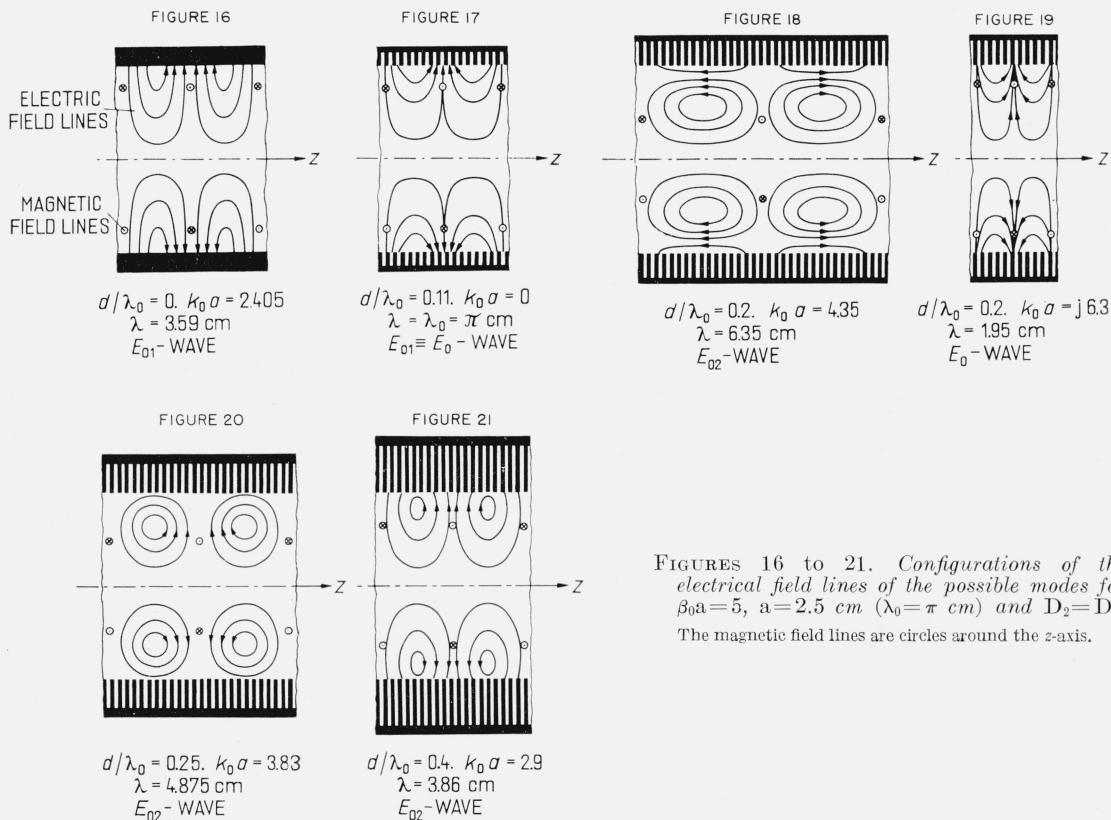
Figure 16 shows the well-known field configuration of the E_{01} -mode in the homogeneous waveguide. The guide wavelength λ exceeds the wavelength λ_0 in space. The electrical field is perpendicular to the surface $r=a$.

In figure 17 there is $d/\lambda_0=0.11$ and $\lambda=\lambda_0$. The electrical field is not perpendicular to the surface $r=a$.

The figures 18 and 19 show the field configurations with $d/\lambda_0=0.2$. Two solutions exist here for $k_0 a$, i.e., one for the E_{02} -mode and one for the E_0 -mode. With the E_{02} -mode there is $\lambda=6.35$ cm, hence more than λ_0 (fig. 18) and with the E_0 -mode there is $\lambda=1.95$ cm, hence less than λ_0 (delay line, fig. 19). Figure 18 does not represent the full field configuration of the E_{02} -mode in the homogeneous waveguide; the electrical field is here not perpendicular to the surface $r=a$. Figure 19 is similar to figure 17, but the wavelength is smaller.

Figure 20 shows the field configuration with $d/\lambda_0=0.25$. The eigenvalue $k_0 a$ is again associated with the E_{02} -mode and is 3.83. The wavelength is therefore $\lambda=4.88$ cm and thus greater than λ_0 . Since the eigenvalue here agrees with that of the H_{01} -mode in the homogeneous waveguide, the electrical field configuration is here the same as that of the magnetic field with the H_{01} -mode.

Figure 21 shows the field configuration with $d/\lambda_0=0.4$. The wavelength is $\lambda=3.86$ cm.



FIGURES 16 to 21. Configurations of the electrical field lines of the possible modes for $\beta_0 a = 5$, $a = 2.5$ cm ($\lambda_0 = \pi$ cm) and $D_2 = D_1$. The magnetic field lines are circles around the z-axis.

The electrical field is perpendicular to the surface $r=0.83a$, but no longer perpendicular to the surface $r=a$.

With the corrugated waveguide, which is often used in practice as a flexible guide section, $\beta_0 d$ always is very small. The eigenvalues $k_0 a$ therefore are near the eigenvalues χ_{0n} .

Corresponding to eq (13) there is then equated $k_0 a = \chi_{0n} + \Theta_E$. With $\epsilon_t = \epsilon_0$ and $\kappa \rightarrow \infty$ eq (20) yields

$$\Theta_E = -\frac{\beta_0 a}{\chi_{0n}} \frac{D_1}{D_1 + D_2} \tan \beta_0 d. \quad (81)$$

This reveals that a corrugated waveguide with the inner radius a has for the E_{0n} modes the same propagating constant and therefore the same field characteristic impedance as a homogeneous waveguide with the inner radius a^* , if

$$a = a^* \left(1 - \frac{\beta_0 a}{\chi_{0n}^2} \frac{D_1}{D_1 + D_2} \tan \beta_0 d \right). \quad (82)$$

If, for instance, $a = 2.5$ cm, $d = 0.1$ cm, $\lambda_0 = 4$ cm ($\beta_0 a = 3.93$), $D_1 = D_2$ there results for the E_{01} -mode $a = 0.946a^*$.

7. Appendix. Equation for Calculation of the Eigenvalue $k_0 a$

According to [7] part B, eqs (18) to (20) the following equation results with the ring-element guide for calculation of the eigenvalue $k_0 a$

$$\frac{k_E \epsilon_0}{k_0 \epsilon_z} \frac{J'_m(k_0 a)}{J_m(k_0 a)} + \frac{k_E \left[\frac{m\gamma}{a} \left(\frac{1}{k_0^2} - \frac{\mu_0}{\mu_p k_H^2} \right) \right]^2}{\omega^2 \mu_0 \epsilon_z \left[\frac{1}{k_0} \frac{J'_m(k_0 a)}{J_m(k_0 a)} + \frac{j}{k_H} \right]} = \frac{H_m^{(2)'}(p_E a) [PH_m^{(1)}(p_E b) - H_m^{(1)'}(p_E b)] + H_m^{(1)'}(p_E a) [H_m^{(2)'}(p_E b) - PH_m^{(2)}(p_E b)]}{H_m^{(2)}(p_E a) [PH_m^{(1)}(p_E b) - H_m^{(1)'}(p_E b)] + H_m^{(1)}(p_E a) [H_m^{(2)'}(p_E b) - PH_m^{(2)}(p_E b)]}, \quad (83)$$

$$P = \frac{k_E \epsilon}{k_2 \epsilon_z} \frac{H_m^{(1)'}(k_2 b)}{H_m^{(1)}(k_2 b)} + \frac{k_E \left[\frac{m\gamma}{b} \left(\frac{1}{k_2^2} - \frac{\mu_0}{\mu_p k_H^2} \right) \right]^2}{\omega^2 \mu \epsilon_z \left[\frac{1}{k_2} \frac{H_m^{(1)'}(k_2 b)}{H_m^{(1)}(k_2 b)} - \frac{j}{k_H} \frac{\mu_0}{\mu} \right]} \quad m=0, 1, 2, \text{ etc.} \quad (84)$$

where

$$k_H = (1-j) \sqrt{\frac{\omega \mu_0 \kappa_p}{2}}. \quad (85)$$

In the following the quantities $\mu_0/(\mu_p k_H^2)$ are neglected with respect to $1/k_0^2$ and $1/k_2^2$. With

$$|p_E a| \gg \begin{cases} 1 \\ m, \end{cases} \quad m=0, 1, 2, \text{ etc.} \quad (86)$$

there results then from the eqs (83) and (84)

$$\left(\frac{m\gamma}{k_0^2 a} \right)^2 = - \left[\frac{\beta_0}{k_0} \frac{J'_m(k_0 a)}{J_m(k_0 a)} + j \frac{Z_H}{Z_0} \right] \left[\frac{\beta_0}{k_0} \frac{J'_m(k_0 a)}{J_m(k_0 a)} + j \frac{Z_0}{Z_a} \right] \quad m=0, 1, 2, \text{ etc.} \quad (87)$$

where

$$\frac{Z_a}{Z_0} = j \frac{Z_E}{Z_0} \frac{P \tan p_E d - 1}{P + \tan p_E d}. \quad (88)$$

Under the assumption of the inequality (15) eq (27) is obtained from eq (88).

The eqs (83) and (84) yield

$$\left(\frac{m\gamma}{k_2^2 b}\right)^2 = -\left[\frac{\beta_2}{k_2} \frac{H_m^{(1)'}(k_2 b)}{H_m^{(1)}(k_2 b)} - j \frac{Z_H}{Z}\right] \left[\frac{\beta_2}{k_2} \frac{H_m^{(1)'}(k_2 b)}{H_m^{(1)}(k_2 b)} - j \frac{Z}{Z_i}\right] \quad \text{for } a \rightarrow 0, m=0, 1, 2, \text{ etc.} \quad (89)$$

where

$$\beta_2 = \beta_0 \sqrt{\frac{\mu\epsilon}{\mu_0\epsilon_0}}, \quad (90)$$

$$Z = \sqrt{\frac{\mu}{\epsilon}}, \quad (91)$$

$$Z_i = jZ_E \frac{J_m(p_E b)}{J'_m(p_E b)}. \quad (92)$$

A very similar equation may be obtained from the results of Wait [11] for a corrugated cylinder excited by a dipole.

8. Principal Symbols

ϵ_0 = dielectric constant of space,

μ_0 = permeability of space,

$Z_0 = \sqrt{\mu_0/\epsilon_0}$ = field impedance of space,

ϵ_i = dielectric constant of the dielectric in the corrugations,

ϵ = dielectric constant of the surrounding medium (can be complex),

μ = permeability of the surrounding medium (can be complex),

κ = conductivity of the metal,

a = inner radius of the guide,

b = outer radius of the guide,

$d = b - a$ = depth of the corrugations,

D_1 = width of the corrugations,

D_2 = spacing of the corrugations,

$D_1 + D_2$ = corrugation constant (analog to optics),

λ_0 = wavelength of a plane wave in space,

λ = wavelength of the guide modes,

$\beta_0 = \frac{2\pi}{\lambda_0}$ = phase constant of a plane wave in space,

$\gamma \equiv \pm j(\beta - j\alpha) = \pm j\beta_0 \sqrt{1 - (k_0/\beta_0)^2}$ = axial propagation constant of the waves on the guide,

$\beta = \frac{2\pi}{\lambda}$ = phase constant,

α = attenuation constant,

f = frequency,

$\omega = 2\pi f$ = angular frequency,

ϑ = equivalent thickness of the conducting layer of the metal,

r, φ, z = cylindrical coordinates,

v_p = phase velocity,

c = velocity of light,

$k_0 a$ = eigenvalue associated with the respective mode,

χ_{mn} = eigenvalue associated with the E_{mn} -mode in a lossless circular waveguide, i.e.,
 n -th not disappearing root of $J_m(\rho)$,

σ_{mn} = eigenvalue associated with the H_{mn} -mode in a lossless circular waveguide, i.e.,
 n -th not disappearing root of $J'_m(\rho)$,

J_m = Bessel function of m -th order,

J'_m = derivative of the Bessel function with respect to the argument,

$H_m^{(1)}$ = Hankel function of first kind and m -th order,

$H_m^{(2)}$ = Hankel function of second kind and m -th order,

$H_m^{(1)'}$, $H_m^{(2)'}$ = derivatives, with respect to the argument, of the Hankel functions of 1st and
2d kind,

$$p_E = k_E - js_E,$$

$$k_E = \beta_0 \sqrt{\epsilon_i / \epsilon_0},$$

$$s_E = \frac{1}{Z_0 D_1} \sqrt{\frac{\omega \mu_0}{2\kappa}} \sqrt{\frac{\epsilon_i}{\epsilon_0}}.$$

$$1N = \text{neper} = 8.7 \text{ db.}$$

9. References

- [1] F. E. Borgnis and C. H. Papas, Electromagnetic waveguides and resonators in encyclopedia of physics, edited by S. Flügge, Vol. XVI, Electric fields and waves, Springer-Verlag, Berlin-Göttingen-Heidelberg, p. 380-389 (1958).
- [2] C. C. Cutler, Bell Telephone Lab. Rept. No. M M 44-160-218 (1944).
- [3] E. L. Chu and W. W. Hansen, The theory of disk-loaded wave guides, J. Appl. Phys. **18**, 996 (1947).
- [4] L. Brillouin, Wave guides for slow waves, J. Appl. Phys. **19**, 1023 (1948).
- 5a] W. Rotman, A study of single-surface corrugated guides, Proc. IRE **39**, 952 (1951).
- 5b] J. R. Wait, Excitation of surface waves on conducting, stratified, dielectric-clad, and corrugated surfaces, J. Research NBS **59**, 365 (1957) RP 2807.
- [6] G. Piefke, Wellenausbreitung in der Scheiben-Leitung, Arch. elektr. Übertrag. **11**, 49 (1957).
- [7] G. Piefke, Die Übertragungseigenschaften einer Leitung aus axial angeordneten, voneinander isolierten Metallringen, Arch. elektr. Übertrag. **11**, 423 and 449 (1957).
- [8] G. Piefke, Wellenausbreitung in einem Blenden-Hohlleiter und einem gesiekten Hohlleiter, Arch. elektr. Übertrag. **12**, 26 (1958).
- [9] G. Piefke, The transmission characteristics of a corrugated guide, IRE Trans. PGAP, **AP-7**, 183 (1959).
- [10] D. Marcuse, Über eine neuartige Oberflächen-Wellenleitung mit Bandpasseigenschaften, Arch. elektr. Übertrag. **11**, 146 (1957).
- [11] J. R. Wait, Radiation from an electric dipole in the presence of a corrugated cylinder, Appl. Sci. Research, **B6**, 117 (1955).

(Paper 64D 4-92)